

## Fluctuations and scaling in aggregation phenomena

C. Ratsch\*

*HRL Laboratories LLC, 3011 Malibu Canyon Road, Malibu, California 90265  
and Department of Mathematics, University of California, Los Angeles, California 90095-1555*

M. F. Gyure

*HRL Laboratories LLC, 3011 Malibu Canyon Road, Malibu, California 90265*

S. Chen and M. Kang

*Department of Mathematics, University of California, Los Angeles, California 90095-1555*

D. D. Vvedensky<sup>†</sup>

*HRL Laboratories LLC, 3011 Malibu Canyon Road, Malibu, California 90265  
and Department of Mathematics, University of California, Los Angeles, California 90095-1555*

(Received 14 January 2000)

We introduce a method which enables us to isolate different sources of fluctuations during a typical aggregation process. As an example, we focus on the evolution of islands during irreversible submonolayer epitaxy. We show that only spatial fluctuations in island nucleation are required to produce the scaling of their size distribution as determined by Monte Carlo simulations. In particular, once the islands are seeded, their growth can be described in a purely deterministic manner.

Many physical phenomena are governed by the aggregation of material. Such processes have been studied in earnest since the early parts of this century<sup>1</sup> and continue to attract considerable interest within areas that range from astrophysics<sup>2</sup> to biology.<sup>3,4</sup> The most powerful methods for analyzing these phenomena are based on general scaling arguments<sup>5</sup> applied to the number and size distribution of the accreting objects. This scaling theory is supported by analytic solutions of mean-field rate equations<sup>6–8</sup> and kinetic Monte Carlo (KMC) simulations.<sup>9,10</sup>

However, these methods do not provide a way of systematically addressing the physical factors that determine scaling behavior. The reason for this can be traced to the complex nature of aggregation phenomena, which typically consist of a nucleation regime, when new objects are created, followed by an aggregation regime as these objects grow by accreting matter from their surroundings. Since both nucleation and growth are due to microscopic processes which are inherently statistical in nature, it is difficult to ascertain *a priori* which aspects of either are intrinsically stochastic and which are essentially deterministic. This has proven to be a major obstacle in the quest for a simple, yet physically realistic, model for aggregation phenomena, where it is essential to understand which aspects of nucleation and growth can be described only by including the appropriate fluctuations.

In this paper, we introduce a model which allows us to address the foregoing issues by examining the effects of individual sources of fluctuations for a prototypical aggregation phenomenon, irreversible submonolayer epitaxy. Our model is based on the level-set method,<sup>11,12</sup> which is a general technique for simulating the motion of moving boundaries. As applied to epitaxial growth,<sup>13</sup> this method solves the Stefan problem for moving island boundaries in the presence of the adatom diffusion field while accommodating the

topological changes caused by nucleation and any coalescence. The analytical framework of our model is ideally suited to the task at hand and, moreover, allows us to ask new questions about the roles of various fluctuations in different regimes of growth.

Submonolayer epitaxial growth is a problem of considerable practical importance in its own right because the surface morphology and, specifically, the size distribution of islands in this regime forms a template for the multilayer surface morphology.<sup>14</sup> The basic scenario of epitaxial growth, e.g., by molecular-beam epitaxy, involves the deposition of atoms onto a substrate with flux  $F$  and the subsequent diffusion of these atoms with diffusion coefficient  $D$  until they either participate in the nucleation of new islands or attach to existing islands. For irreversible aggregation, a central quantity which characterizes the morphology of the surface is the ratio  $D/F$ . In particular, in the limit  $D/F \rightarrow \infty$  (the scaling limit), the distribution of island sizes can be expressed in terms of a universal function.<sup>5,9</sup> The main purpose of this paper is to identify the fluctuations which are relevant in this limit.

A model that correctly describes the spatial and temporal fluctuations of the adatom concentration, due to deposition and migration, implicitly captures all fluctuations. Such microscopic models, usually based on KMC methods, have reproduced many aspects of submonolayer epitaxy for a variety of experimental scenarios, especially island size distributions.<sup>10,15</sup> In a more “coarse-grained” model, however, only the positioning of islands and subsequent evolution of their boundaries are of interest. To build such a conceptually simpler model, it is necessary to focus on the fluctuations in nucleation and growth apart from those in the adatom concentration. This would be difficult, if not impos-

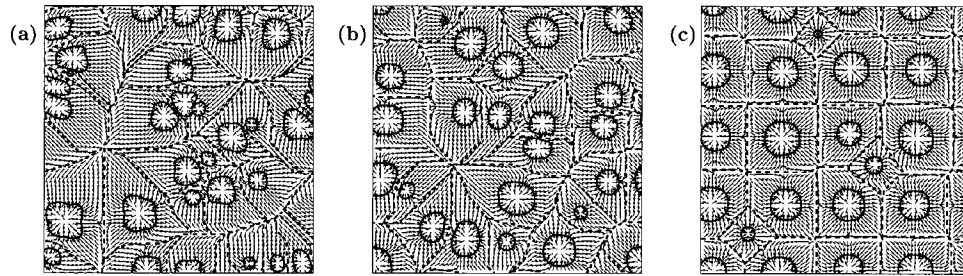


FIG. 1. Typical surface morphologies (solid lines) at a coverage of 0.2 monolayers (ML) using the random (a), probabilistic (b), and deterministic (c) seeding style. The results were obtained on a square lattice of size  $L/a=90$ , and with  $D/F=10^6$ . The capture zone boundaries (dashed lines) were obtained by separating the domains of attraction, where the arrows point in the direction of the gradient of the diffusion field.

sible, to carry out using typical KMC simulations because they are based on stochastic transition rules for single atoms.

Here, we isolate spatial and temporal fluctuations in the nucleation and growth of islands, and discuss each individually. We find that only spatial fluctuations in the seeding of new islands, suitably weighted by the adatom density, are required to produce the correct scaling form of the island-size distribution, as determined by KMC simulations. No other fluctuations are required to produce this scaling form.

The central constructs of our model are a spatially varying adatom density and the creation and motion of island boundaries by the level set method. The main idea behind this method<sup>11,12</sup> is that a (zero thickness) boundary curve, such as the boundary of an island, can be represented by the set  $\varphi = 0$ , called the *level set*, of a smooth function  $\varphi$ , the level set function. For a given boundary, this function evolves according to

$$\frac{\partial \varphi}{\partial t} + \mathbf{v} \cdot \nabla \varphi = 0, \quad (1)$$

where  $\mathbf{v}$  is the boundary velocity. All physical information about the boundary motion is contained in the normal component  $v_n = \mathbf{n} \cdot \mathbf{v}$ , where  $\mathbf{n}$  is the outward normal of the moving boundary and  $\mathbf{v} \cdot \nabla \varphi = v_n |\nabla \varphi|$ . For the case of irreversible aggregation,  $v_n$  is computed as

$$v_n = a^2 D (\mathbf{n} \cdot \nabla \rho^- - \mathbf{n} \cdot \nabla \rho^+), \quad (2)$$

where  $a$  is the lattice constant,  $\rho$  is the adatom density, and the superscripts label the contributions from above (+) and below (-) the boundary. The adatom density is obtained by numerically integrating the diffusion equation

$$\frac{\partial \rho}{\partial t} = F + D \nabla^2 \rho - 2 \frac{dN}{dt}, \quad (3)$$

with the condition that  $\rho = 0$  at all island boundaries and where  $N$  is the island density. The last term accounts for the loss of adatoms due to the nucleation of dimers, which are the smallest stable islands,

$$\frac{dN}{dt} = D \sigma_1 \langle \rho^2 \rangle, \quad (4)$$

where  $\langle \cdot \rangle$  denotes the spatial average of  $\rho(\mathbf{x}, t)^2$  and  $\sigma_1$  is the adatom capture number.<sup>17</sup> The square of the adatom density is used because two adatoms are needed at the same

position to form a dimer. The validity of the nucleation rate given by Eq. (4) has been shown in Ref. 17.

The model, as described by Eqs. (1)–(4), is not yet complete because we have not specified whether the flux and diffusion field are stochastic or deterministic, nor have we specified how new boundaries are created through nucleation and incorporated into the level set function. The accommodation of new boundaries within the level set function is accomplished generically by adding to the right-hand side of Eq. (1) a source term of the form  $\sum_n \delta(t - t_n) \delta(\mathbf{x} - \mathbf{x}_n)$  to account for nucleation events which occur at times  $t_n$  and at positions  $\mathbf{x}_n$ . The structure of these equations implies that any fluctuations (spatial or temporal) in either the adatom density or flux produces only temporal fluctuations in the nucleation rate, because a spatial average of  $\rho(\mathbf{x}, t)^2$  is taken in Eq. (4). We seed the  $n$ th island at time  $t_n$  defined by the number of islands  $NL^2$  passing the integer value  $n$ , where  $L$  is the system size. The justification for this deterministic treatment of nucleation *times* will be provided below.

Equations (1)–(4) allow complete freedom for the *spatial* dependence of nucleation. We discuss three styles, which we refer to as random, probabilistic, and deterministic. For random seeding, nucleation can occur on any lattice site with equal likelihood. This clearly takes no account of spatial variations in the adatom density. Since two atoms are needed to nucleate a new island [cf. Eq. (4)], another plausible choice is to weight the position of a new island by the local value of  $\rho^2$ . We call this the probabilistic seeding style. We will also discuss deterministic seeding where islands are always seeded at the point where  $\rho$  has its maximum value. In fact, in our model, it is easy to use a probability that is weighted by any power of  $\rho$ , as computed from Eq. (3). Our seeding styles correspond to  $\rho^0$  (random),  $\rho^2$  (probabilistic), and  $\rho^\infty$  (deterministic).

Typical surface morphologies for the different seeding styles are shown in Fig. 1. Increasing the power in the weighting clearly leads to a more regular distribution of islands. This can also be seen in Fig. 2, where we show scaling plots<sup>9</sup> of the corresponding island size distributions. The distribution function produced by the deterministic seeding style exhibits a pronounced peak with a sharp drop off for large islands. As is evident in Fig. 1, islands are always seeded as far away as possible from existing islands, because this is where the adatom concentration is highest. This has the effect of diminishing the competition between neighboring islands for adatom capture, so many islands grow to approximately the same size.

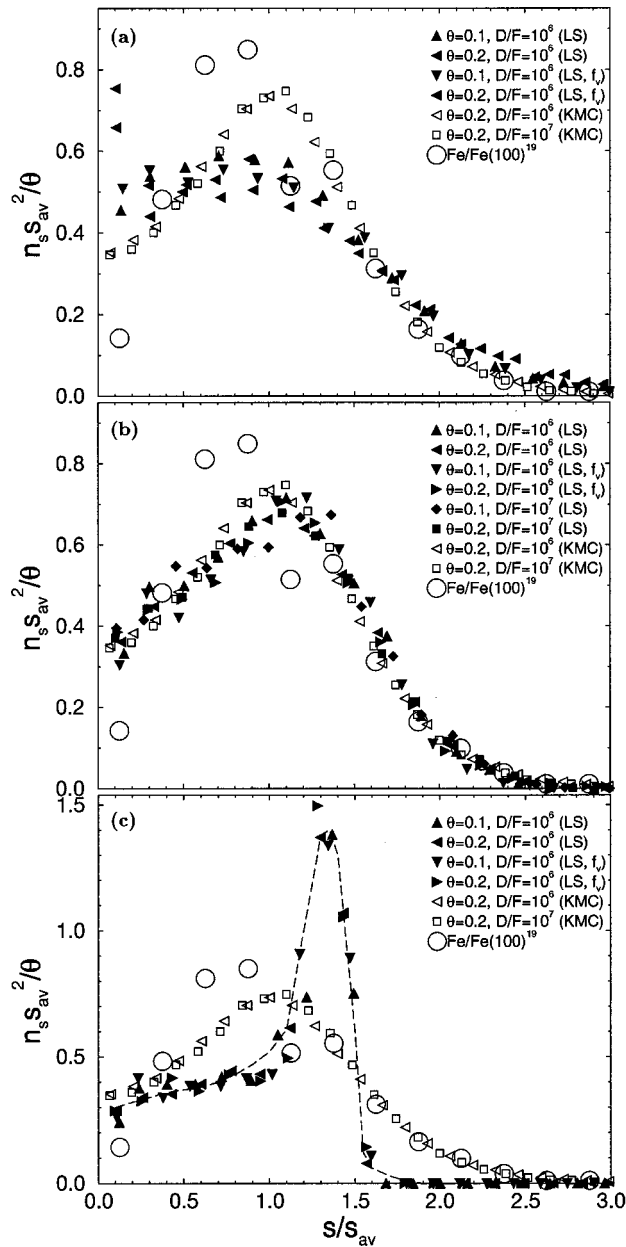


FIG. 2. Comparison of scaled island-size distributions, where  $n_s$  is the number of islands of size  $s$ ,  $s_{av}$  is the average island size, and  $\theta$  is the coverage. The data for random (a) and probabilistic (b) seeding represents an average over at least 50 independent lattices, with  $L/a=180$ , and a numerical grid of linear size 512. This leads to a standard deviation that is always  $\leq 0.05$ . The data for deterministic (c) seeding was obtained with  $L/a=360$ , and a numerical grid of linear size 1024. Here, the standard deviation ranges from 0.1 to 0.2. Note the different scale of panel (c). Also shown is data with fluctuations in the growth velocity (denoted by  $f_v$ ), as described in the text. All level-set (LS) data is denoted by closed symbols. The dashed line in panel (c) is a guide to the eye. The KMC data (open symbols) are the average of 8 runs on a  $2000 \times 2000$  lattice. Edge diffusion was included in the simulation to obtain compact island shapes. Experimental data (big open circles) for Fe/Fe(100) (Ref. 18) is also shown in each panel.

As the seeding becomes more random, some islands have a larger probability to be seeded next to existing islands, thus inhibiting their growth, while others will have few neighboring islands, and thus grow faster. Therefore, the size distribution

broadens, as observed in Fig. 2. Another trend which is evident in Fig. 1 is that the island density increases with increasing randomness. This is because the overall efficiency of adatom capture by islands decreases. With greater randomness in seeding, it becomes more likely to nucleate near an existing island. Therefore the adatom density increases leading to a corresponding increase in the nucleation rate. Nevertheless we obtain the well-known scaling law<sup>16</sup>  $N \sim (D/F)^{-1/3}$  for all seeding styles (not shown).

We have chosen the time of nucleation events deterministically, as given by Eq. (4). We can now understand why this is justified. With increasing  $D/F$ , there is a greater tendency for the nucleation of all islands to occur at earlier times. Thus, the time intervals between successive nucleation events decrease, so islands grow very little between successive nucleation events. Substantial island growth occurs only after nucleation has almost completed. Therefore, any temporal fluctuations in the seeding will have very little influence on the size of an island. All that appears to be relevant is the spatial correlation of island positions, which is accounted for by the spatial fluctuations in the seeding.

The vastly different shapes of the distribution functions invite comparison to data obtained from KMC simulations and from experiment. In Fig. 2 we also compare the scaled island-size distribution functions with the different seeding styles to that obtained from KMC simulations. The agreement between the distributions generated by the probabilistic seeding and those from the KMC simulations is quite striking. Probabilistic seeding also gives an acceptable account of experimental data<sup>18</sup> for Fe/Fe(001) [Fig. 2(b)]. Moreover, we obtain excellent data collapse of the distribution functions for different coverages and different values of  $D/F$ , as also shown in Fig. 2(b).

According to Eq. (2), the motion of island boundaries is deterministic for *any* seeding style if  $F$  and  $\rho$  are deterministic. But, in general, fluctuations in the adatom density can also result in fluctuations in the growth velocity of the island boundaries. We have therefore also tested a nonconservative fluctuation for  $v_n$ , where at every timestep we multiply the velocity calculated from Eq. (2) by a random number between 0.5 and 1.5. Results with these fluctuations for all seeding styles are also shown in Fig. 2. These additional fluctuations have no effect because they can be averaged, while the spatial fluctuations in the seeding cannot. This can be understood as follows: Once a ‘‘mistake’’ is made in the choice of the location of a new island, it cannot be corrected, while a fluctuation in the growth of an island boundary can be corrected over time. We thus conclude that once the islands are seeded the island boundaries can be evolved in a purely deterministic fashion.

The strong qualitative differences between the island-size distributions obtained with the different seeding styles implies that spatial fluctuations in the seeding of new islands are an essential ingredient of any model. This is ultimately the reason why standard mean-field rate equations do not reproduce the correct island-size distribution. The spatial information of the local environment of each island is necessary for the correct evolution of the surface morphology and is a direct consequence of the spatial fluctuations in the seeding of islands. This can be illustrated by examining the domains of attraction of the adatom diffusion field associated

with the islands (Fig. 1). These “capture zones” provide a direct indication of the growth rate of an island.<sup>7,19</sup> It is immediately apparent from Fig. 1 that the deterministic seeding style leads to a much more regular distribution of capture zones, which is why the islands have a much more regular size distribution. It is interesting to note that this size distribution is qualitatively very similar to that obtained from a model where the velocity is assumed to be spatially constant.<sup>13</sup> The placement of new islands in the deterministic seeding style has the effect of eliminating (almost) all spatial information because all the islands have (almost) identical local environments.

Finally, we discuss the effect of fluctuations on scaling. From the quality of the data collapse in Fig. 2, we conclude that our model has attained its scaling limit. From the results produced by all the fluctuations considered, we further conclude that only spatial fluctuations in island seeding are rel-

evant in this limit. Other fluctuations will be important in the pre-asymptotic regime, but our results suggest that these effects are small for typical values of  $D/F$  ( $\geq 10^5$ ).

Quite apart from the specific results presented here, we stress that our methodology allows us to ask questions and address issues that were previously difficult, if not impossible, to pursue with established methods. We believe that new avenues of investigation into the relevance of different types of fluctuations in various regimes of aggregation phenomena may be opened by considering simpler models that encapsulate the essential features of this model.

We acknowledge many helpful discussions with R. Caflich, B. Merriman, and S. Osher. This work was supported by the NSF and DARPA through Cooperative Agreement No. DMS-9615854 as part of the Virtual Integrated Prototyping Initiative.

\*Author to whom correspondence should be addressed. Electronic address: cratsch@math.ucla.edu

<sup>†</sup>Permanent address: The Blackett Laboratory, Imperial College, London SW7 2BZ, United Kingdom.

<sup>1</sup>M. von Smoluchowski, Phys. Z. **17**, 583 (1916).

<sup>2</sup>J. Peacock, Mon. Not. R. Astron. Soc. **284**, 885 (1997).

<sup>3</sup>H.E. Stanley, S.V. Buldyrev, L. Cruz, T. Gomez-Isla, S. Havlin, B.T. Hyman, R. Knowles, B. Urbanc, and C. Wyart, Physica A **249**, 460 (1998).

<sup>4</sup>L.T. Perelman, V. Backman, M. Wallace, G. Zonios, R. Manoharan, A. Nusrat, S. Shields, M. Seiler, C. Lima, T. Hamano, I. Itzkan, J. Van Dam, J.M. Crawford, and M.S. Feld, Phys. Rev. Lett. **80**, 627 (1998).

<sup>5</sup>T. Vicsek and F. Family, Phys. Rev. Lett. **52**, 1669 (1984).

<sup>6</sup>P.G.J. van Dongen and M.H. Ernst, Phys. Rev. Lett. **54**, 1396 (1985); P.G.J. van Dongen, *ibid.* **63**, 1281 (1989).

<sup>7</sup>M.C. Bartelt and J.W. Evans, Phys. Rev. B **54**, R17 359 (1996).

<sup>8</sup>D. Kandel, Phys. Rev. Lett. **79**, 4238 (1997).

<sup>9</sup>M.C. Bartelt and J.W. Evans, Phys. Rev. B **46**, 12 675 (1992); J.

W Evans and M.C. Bartelt, J. Vac. Sci. Technol. A **12**, 1800 (1994).

<sup>10</sup>C. Ratsch, P. Šmilauer, A. Zangwill, and D.D. Vvedensky, Surf. Sci. Lett. **329**, L599 (1995).

<sup>11</sup>S. Osher and J.A. Sethian, J. Comput. Phys. **79**, 12 (1988).

<sup>12</sup>S. Chen, B. Merriman, S. Osher, and P. Smereka, J. Comput. Phys. **135**, 8 (1997).

<sup>13</sup>M.F. Gyure, C. Ratsch, B. Merriman, R.E. Caflich, S. Osher, J.J. Zinck, and D.D. Vvedensky, Phys. Rev. E **58**, R6927 (1998).

<sup>14</sup>E. Somfai, D.E. Wolf, and J. Kertesz, J. Phys. I **6**, 393 (1996).

<sup>15</sup>J.G. Amar and F. Family, Thin Solid Films **272**, 208 (1996).

<sup>16</sup>J.A. Venables, G.D.T. Spiller, and M. Hanbücken, Rep. Prog. Phys. **47**, 399 (1984).

<sup>17</sup>G.S. Bales and D.C. Chrzan, Phys. Rev. B **50**, 6057 (1994).

<sup>18</sup>J.A. Stroschio and D.T. Pierce, Phys. Rev. B **49**, 8522 (1994).

<sup>19</sup>P.A. Mulheran and J.A. Blackman, Philos. Mag. Lett. **72**, 55 (1995); P.A. Mulheran and J.A. Blackman, Phys. Rev. B **53**, 10 261 (1996).